

Ordering magnetic dipole moments in resonant dielectric metasurfaces

Pengchao Yu¹, Vladimir R. Tuz^{2,3}, Victor Dmitriev⁴, and Yuri S. Kivshar⁵

¹*College of Physics, Jilin University, Changchun 130012, China*

²*International Center of Future Science, State Key Laboratory of Integrated Optoelectronics, College of Electronic Science and Engineering, Jilin University, 2699 Qianjin Street, Changchun 130012, China*

³*Institute of Radio Astronomy, National Academy of Science of the Ukraine, Kharkiv 61002, Ukraine*

⁴*Electrical Engineering Department, Federal University of Para,*

PO Box 8619, Agencia UFPA, CEP 66075-900 Belem, Para, Brazil and

⁵*Nonlinear Physics Center, Australian National University, Canberra ACT 2601, Australia*

(Dated: September 2, 2022)

Artificial magnetism at optical frequencies can be realized in metamaterials composed of periodic arrays of subwavelength elements (meta-atoms). Here we demonstrate that optically-induced magnetic moments can be arranged in both *ferromagnetic* (FM) and *antiferromagnetic* (AFM) orders in low-symmetry all-dielectric Mie-resonant metasurfaces where each meta-atom supports a localized trapped mode. We reveal that such metasurfaces possess not only strong optical magnetic response but also demonstrate significant polarization rotation of the normally incident linearly polarized waves at both AFM and FM resonances. We confirm these features theoretically and experimentally by measuring directly the spectral characteristics of different modes excited in a dielectric metasurface, and mapping near-field patterns of the electromagnetic fields at the microwave frequencies.

I. INTRODUCTION

Natural materials exhibit negligible magnetism at optical frequencies because direct effects of optical magnetic fields on matter are much weaker than the effects of electric fields [1]. A lack of strong optical magnetism in natural materials has motivated many researchers to search for various strategies for achieving a strong magnetic response in specially engineered nanostructures and metamaterials. Even being made of non-magnetic constituents, metamaterials can possess many characteristics of magnetic materials being driven by optically-induced magnetic moments. For example, their effective permeability tensor differs from the unity tensor because of specifically chosen form and arrangement of the subwavelength particles (often called ‘meta-atoms’). In general, an array of meta-atoms responds to the electromagnetic waves as an effective medium demonstrating a dynamic resonant magnetic response (see comprehensive reviews of artificial magnetism in Refs. [2–4]).

Several designs of meta-atoms have been proposed to achieve the artificial magnetism. A canonical example of the corresponding meta-atom is a metallic split-ring resonator (SRR). If many of such resonators are arranged in a two-dimensional array, they form a metasurface. In the metasurface illuminated by an external electromagnetic wave, magnetic dipole moments arise from the circular current flow induced in the particles’ material. Such a mechanism of attaining the artificial magnetism was first demonstrated at microwave frequencies [5], and then it was extended to optics by exploiting the plasmonic resonances of metallic nanoparticles [6–9]. It has been developed further for a variety of non-magnetic plasmonic structures ranging from nanobars and nanoparticle clusters [10–13] to more complicated systems [14–16].

However, it becomes clear that plasmonic metasurfaces

based on arrays of metallic SRRs cannot support strong optical magnetism above 100 THz, especially in the visible frequency range, due to conduction of metals [17]. For higher frequencies it was proposed to use subwavelength meta-atoms made of high-index low-loss dielectric materials. Each particle behaves as a dielectric resonator sustaining a set of Mie-type modes [18–20], while their ensemble creates a macroscopic resonant response of the metasurface.

The basic physical mechanism of the artificial magnetism in the dielectric particles is the excitation of the corresponding modes of the resonator with a circular flow of the displacement currents. The spectral position of resonances can be tuned by changing the size of particles employed for meta-atoms. This mechanism has been realized in diverse metasurfaces composed of dielectric nanoparticles for their operating in the entire visible spectral range [18, 21]. Nevertheless, we notice that the resonances arising from the Mie-type modes in all-dielectric metasurfaces do not provide the desirable strong near-field enhancement such as that observed for plasmonic resonances in their metallic counterparts.

In order to achieve strong effective interaction of magnetic dipole moments manifested in the ferromagnetic (FM) and anti-ferromagnetic (AFM) orders at the THz frequencies, a hybrid metal-dielectric structure composed of silicon nanoparticles (spheres) and metallic SRRs was initially suggested [22]. By arranging such hybrid meta-atoms into a two-dimensional lattice, an alternating magnetization in the in-plane directions is obtained due to the magnetic interaction between the dielectric spheres. The appearance of the AFM order in such hybrid metasurface has been confirmed experimentally [23]. This concept has been developed further for all-dielectric metasurfaces composed of ‘diatomic’ meta-atoms of dissimilar Mie-resonant dielectric particles [24].

In this paper, we develop a novel approach to optically-induced magnetic ordering in metamaterials and demonstrate that in all-dielectric metasurfaces composed of clusters of identical particles, both resonant FM and AFM orders can be achieved at different frequencies for the same geometry of metasurface. These dissimilar magnetic resonances arise due to the splitting of the so-called trapped modes excited in each meta-atom with broken in-plane symmetry. Remarkably, at the resonant frequencies of both FM and AFM structured orders of magnetic dipoles, the metasurface demonstrates a strong polarization transformation of the transmitted and reflected waves.

II. CONCEPTUAL FRAMEWORK

We consider all-dielectric metasurfaces supporting trapped (dark) mode resonances which appear in metasurfaces provided that their meta-atoms possess certain structural asymmetry. Recently, the modes influenced by the symmetry breaking in resonators were attributed to the phenomenon of bound states in the continuum (BIC) [25, 26]. The mechanism of excitation of trapped modes was first introduced to metasurfaces composed of thin metallic SRRs and their complimentary patterns [27–29], and then extended on the all-dielectric case [30–34]. Remarkably, such metasurfaces provide a strong localization of the electromagnetic fields depending on the degree of asymmetry of the meta-atom. By choosing a proper design of such asymmetric meta-atoms, one can excite a trapped mode with a circular displacement current flow and, thus, achieve an artificial magnetism.

When the metasurface is made of equidistantly arranged identical meta-atoms, all magnetic moments are oriented equally and orthogonally to the structure plane. This is valid for both types of magnetic dipole moments, either induced in metallic SRRs by the oscillation of free electrons or by the displacement current in dielectric meta-atoms. From the viewpoint of theory of magnetism and magnetic systems, one should identify the order of such out-of-plane magnetic moments as an FM order.

However, when particles are aggregated into clusters, strong nearest-neighbour interactions (coupling) in the metasurface array become dominate, and the mutual magnetization of the neighboring elements can appear in the anti-parallel fashion [35, 36]. The appearance of such dynamic patterns of induced alternating magnetic moments resembles the AFM order. It turned out that AFM order can be easily achieved in the metallic metasurfaces [37, 38], since thin SRRs supporting surface currents can be given a quite complicated shape, while its excitation for optical frequencies with the use of volumetric dielectric resonators supporting displacement currents is not so trivial.

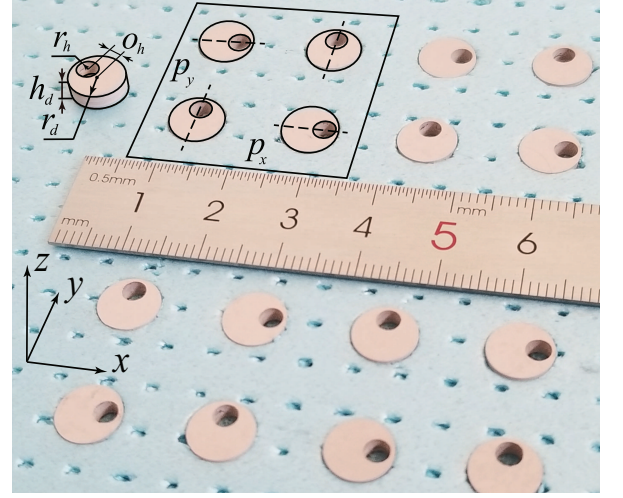


FIG. 1. Schematic view of the low-symmetry metasurface where unit cell with a period $p = p_x = p_y = 32$ mm is outlined. The particles are nonmagnetic ceramic disks with eccentric circular through-holes. They are arranged in a rigid foam holder. Permittivity of ceramic and foam are $\epsilon_d = 20.5$ and $\epsilon_s = 1.05$, respectively. Radius and thickness of the disks are $r_d = 4$ mm and $h_d = 2.5$ mm, respectively. Radius of the hole is $r_h = 1.5$ mm, and the offset of the hole center from the disk center is $o_h = 2$ mm.

III. SPECIFIC REALIZATION

In order to construct a dielectric metasurface supporting strong optically-induced magnetic coupling with magnetic ordering, here we employ a set of identical sub-wavelength particles (Fig. 1). They are cylindrical dielectric resonators (disks). Each disk is perturbed in-plane by an eccentric through-hole. The geometry of such disk belongs to the point group C_s having one mirror plane (we use Schönflies notation for the point groups [39]). Previously it was revealed [32], that in such a perturbed resonator a trapped mode can be excited under the frontal illumination, when the vector of electric field of the incident linearly polarized wave does not coincide with the mirror plane of the perturbed resonator. In terms of the eigenwaves of the cylindrical resonator, this trapped mode corresponds to the lowest transverse electric (TE_{011}) mode of the nonperturbed resonator which features the axial (vertical) magnetic moment (the correspondence between eigenwaves and Mie-type modes of a cylindrical resonator see in Tab. 1 of Ref. [40]). For the metasurface composed of such resonators, when all resonators are arranged equidistantly, all magnetic moments appear to be equally out-of-plane oriented at any instant in time forming the FM order at the resonant frequency of the trapped mode excitation [32].

Let us further outline in the metasurface a square unit cell (cluster) with the lattice period p . This cluster encloses four identical disks with holes. Within the unit cell, each disk can be rotated along its axial axis. The final orientation of the holes thus defines the symmetry

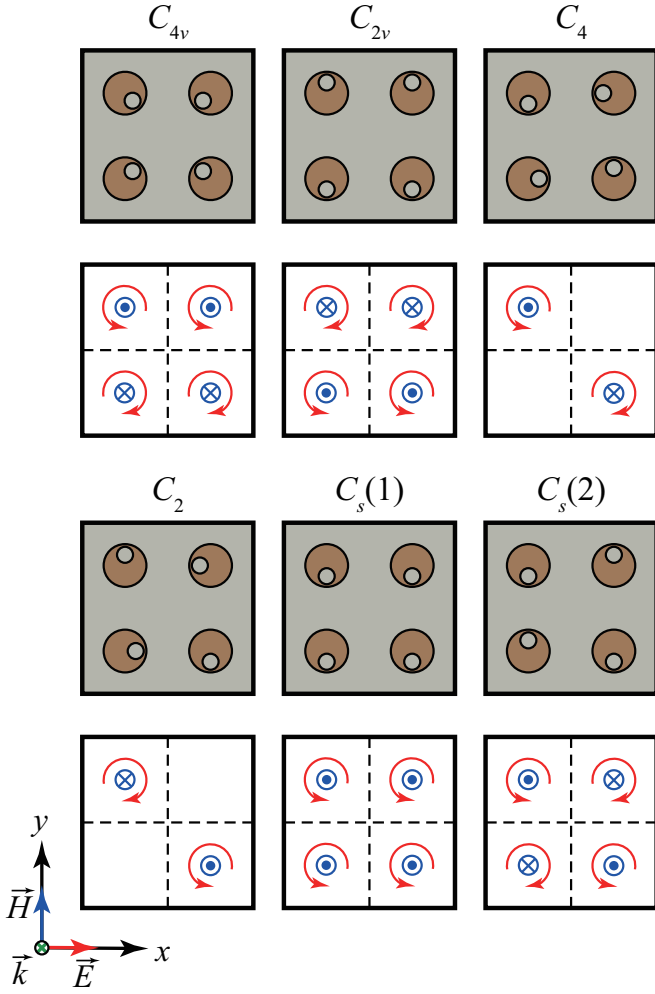


FIG. 2. A set of unit cells of the all-dielectric metasurface and corresponding groups and configurations of displacement currents (red arrows) and out-of-plane magnetic moments (blue bull's eye and crossed circle pictograms).

of the cluster. Further, we exclude the case when all the holes are oriented randomly, and consider only their orientation along the selected axes of symmetry of the square unit cell (see Fig. 3 of Ref. 41). The full list of symmetries for the resulting unit cells is C_{4v} , C_{2v} , C_4 , C_2 , and C_s (see the group subordination scheme (group tree) given in Fig. 2 of Ref. 42).

Figure 2 shows the exhaustive list of possible symmetries of a square unit cell composed of four perturbed disks (enantiomorphic modifications for the groups C_4 and C_2 are not presented here; see also Fig. 3 of Ref. 41). All configurations of displacement currents and out-of-plane magnetic moments are derived for the metasurface illuminated by the horizontal (x -polarized) normally incident plane electromagnetic wave ($\vec{k} = \{0, 0, -k_z\}$). In these schemes empty squares and those having pictograms correspond to the inactive and active resonators, respectively. One can see that only unit cell with symmetry $C_s(1)$ demonstrates a FM order of magnetic mo-

ments, and unit cell with symmetry $C_s(2)$ allows an AFM order with magnetic moments arranged in an alternating staggered pattern.

As soon as such a complex unit cell is constructed, the overall characteristics of the metasurface become to be determined not only by the characteristics of the individual resonators, but also their collective excitation due to coupling in the cluster. Because of this coupling, the appearance of the AFM order is possible. Moreover, it is revealed [41] that the resonators orientation within the unit cell corresponding to the symmetries C_{4v} , C_{2v} , C_4 , and C_2 support the instant antiparallel magnetic moments, whereas only the arrays possessing the symmetry C_s can demonstrate either FM order or AFM order with an alternating pattern of magnetic moments. Remarkably, all arrays support only one kind of magnetization for any linear polarization of the normally incident electromagnetic wave.

Based on this knowledge, we consider a metasurface whose unit cell does not possess symmetry. This unit cell is constructed of two pairs of perturbed disks with the 90-degree difference in the hole rotation between the pairs (Fig. 1). With such an arrangement of disks the unit cell has no symmetry, i.e. it belongs to the group C_1 . In fact, by symmetry, the all-dielectric metasurface under study is a complete analogue of the previously studied metallic (plasmonic) SRR array [35, 36]. It was demonstrated that such array supports both FM and AFM orders which appear due to the coupling effects. Either FM or AFM order arises when the metasurface is illuminated by the wave whose polarization is along either of the two diagonals of the unit cell. In what follows, our goal is to reveal the manifestation of this effect in our all-dielectric metasurface.

As an exciting radiation, we consider a normally incident linearly polarized plane electromagnetic wave. We distinguish polarization of the incident wave with the vector \vec{E} oriented either horizontally (along the x -axis; x -polarization) or vertically (along the y -axis; y -polarization), or along the unit cell diagonals [diagonal d_1 -polarization (left-to-right, bottom-to-top) and diagonal d_2 -polarization (left-to-right, top-to-bottom)]. Relying on the capabilities of our measurement platform, we choose the microwave frequency range (9 – 12 GHz) for our study.

We perform the numerical simulations of the electromagnetic response of the given metasurface with the use of commercial COMSOL Multiphysics® finite-element electromagnetic solver. We have modified Model #15711 from COMSOL Application Gallery [43] and use options of the periodic ports and Floquet periodic boundary conditions of the rf module to simulate the infinite two-dimensional array of dielectric resonators. In our model we set the geometrical and material parameters of the unit cell as listed in the caption of Fig. 1. Initially, the ideal (lossless) metasurface is simulated, then actual material losses are taken into account to match the simulation results with the experimental data. In both cases,

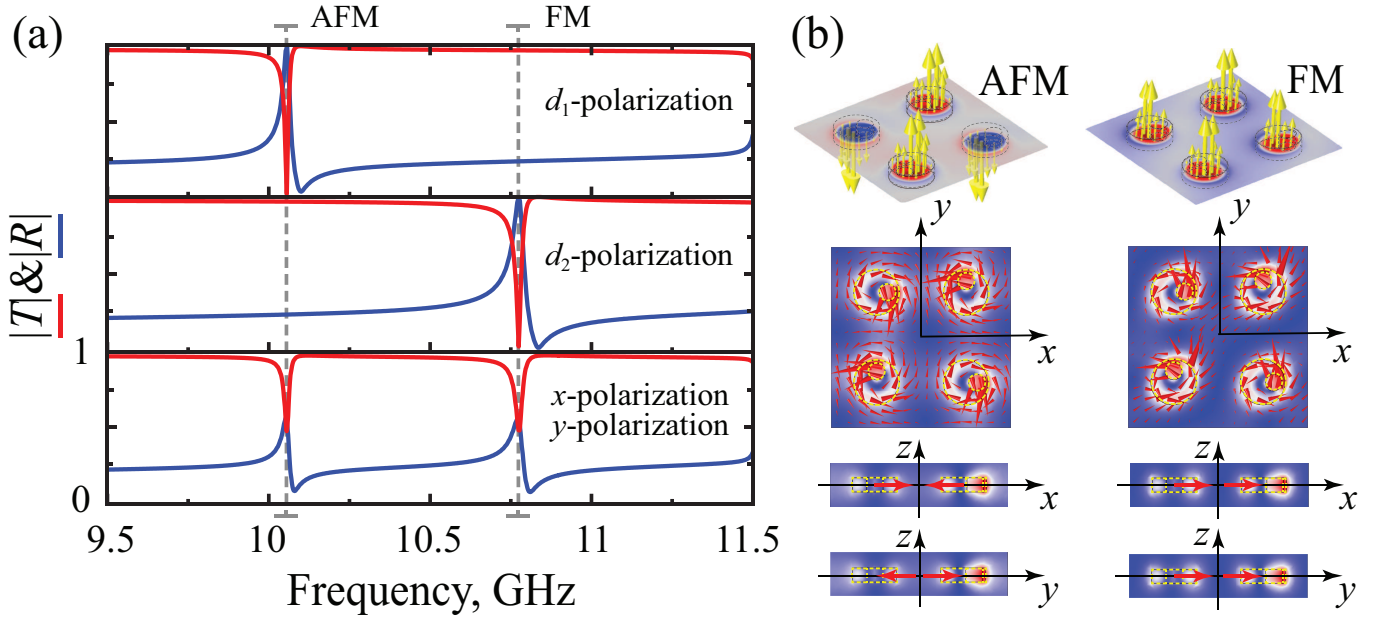


FIG. 3. (a) Simulated transmission and reflection spectra of the ideal (lossless) metasurface excited by a normally incident linearly polarized wave. (b) Distributions of the magnetic field (yellow arrows) and electric field (red arrows) at the frequencies of excitation of the antisymmetric (AFM) and symmetric (FM) resonances. All geometrical and material parameters of the metasurface are the same as in Fig. 1.

the presence of holder is ignored, since its permittivity differs little from the permittivity of free space.

Figure 3(a) shows simulated transmission and reflection spectra of the metasurface illuminated by a normally incident plane wave for its four different linear polarizations. One can see that in the frequency band of interest, the spectra for waves of diagonal polarizations are different, while they are the same for the x - and y -polarized waves. There are the low-frequency resonance and high-frequency resonance in the spectra of the d_1 - and d_2 -polarized waves, respectively, and both resonances are in the spectra of the x - and y -polarized waves.

In order to discover the nature of these resonances we performed the simulation of the electromagnetic near-field distributions at the corresponding resonant frequencies. These simulations are depicted in Fig. 3(b). From this figure one can conclude that at the chosen resonant frequencies all resonators forming the cluster are active ones. In each resonator a particular near-field pattern appears where the arrows of the electric field demonstrate a circular flow in the x - y plane. Such a flow produces magnetic moments in each resonator oriented along its axis (along the z axis). In fact, these resonances arise from the trapped mode of the perturbed cylindrical resonator [32] and they are not excited entirely in the metasurfaces composed of nonperturbed disks [44]. The trapped mode splits into symmetric high-frequency resonance and antisymmetric low-frequency resonance because there is a coupling between the perturbed resonators in the cluster. While for the symmetric resonance the magnetic moments are oriented equally, those for the antisym-

metric resonance are anti-parallel in the adjacent resonators. Therefore, such arrangements of magnetic moments resemble the FM and AFM orders for the high-frequency and low-frequency resonances, respectively (we distinguished corresponding resonant frequencies by letters f_{FM} and f_{AFM}).

IV. EXPERIMENTAL STUDIES

We now proceed to visualization of two above discussed orders of magnetic moments by direct experiment. For plasmonic SRR-based metasurfaces such experiment has been already performed [45] by employing scanning near-field optical microscopy. Further we perform both far-field and near-field microwave measurements to demonstrate manifestation of the FM and AFM orders in our all-dielectric metasurface.

In order to assemble a metasurface prototype for experimental study, a set of dielectric particles was fabricated. As a dielectric material the Taizhou Wangling TP-series microwave ceramic has been used. The dielectric particles with the sizes mentioned in the caption of Fig. 1 were fabricated with the use of precise mechanical cutting techniques. To arrange them into a metasurface prototype, an array of holes was milled in a custom holder made of a rigid foam (Styrofoam) material. The metasurface prototype is composed of 11×11 clusters (so we used 484 particles in total).

At the first step we measured the transmission and reflection spectra of the metasurface prototype. We

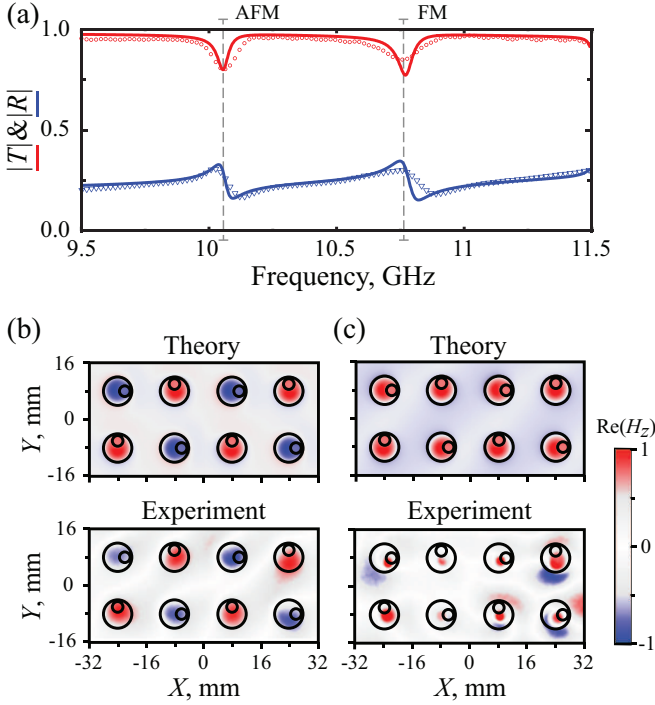


FIG. 4. (a) Simulated (solid lines) and measured (scatters) transmission and reflection spectra, and real part of the normal component (H_z) of the magnetic near-field (out-of-plane magnetic moments) at the frequencies of (b) antisymmetric (AFM) and (c) symmetric (FM) resonances excited by the horizontal (x -polarized) incident wave. Material losses in ceramic are $\tan \delta = 0.015$. All other geometrical and material parameters of the metasurface are the same as in Fig. 1.

used a pair of dielectric-lens antennas (HengDa HD-100LHA250) with a gain of 25 dB over the frequency bandwidth of 8.2 – 12.4 GHz. The antennas are specifically oriented to generate and receive a horizontally linearly polarized wave. The prototype is fixed in the middle between the antennas, where a distance between the antennas is 3 m. The antennas are connected to the corresponding ports of the Keysight E5071C Vector Network Analyzer by standard 50 Ohm coaxial cables. All measurements are performed in an anechoic chamber (details on the experimental setup and measurement technique see in Refs. 34 and 46).

The measured transmission and reflection spectra of the metasurface are depicted in Fig. 4(a). One can see that the curves appeared somewhat smoothed due to the presence of real material losses. We have specified our computational model by accounting material losses existing in ceramic particles. After that, the simulated and measured data are found to be in a good agreement, while their remaining minor deviation can be explained by fabrication imperfection in the actual metasurface prototype. Both resonances predicted by the theory are recognized in the measured spectra, and their resonant frequencies f_{AFM} and f_{FM} coincide in the measured data and simulations.

Next we performed a near-field mapping measurements at the corresponding resonant frequencies f_{AFM} and f_{FM} to obtain a complete confidence in the appearance of specific orders of the magnetic moments.

In the measurement setup, a receiving antenna was substituted by an electrically small magnetic dipole probe (a metallic loop with diameter 3 mm) oriented in parallel to the metasurface plane. Two unit cells (eight particles) were included in the scan area. During the measurements the probe was automatically moved over the scan area on a distance of 1 mm above the prototype surface. The LINBOU near-field imaging system is adopted to perform the movement of probe with a 1 mm step width in each direction. The real part of the normal component (H_z) of the magnetic near-field has been extracted from the measured data and presented in Fig. 4(b). In this figure the measured data are supplemented by the corresponding simulated patterns.

The resulting measured and simulated patterns match each other. Obviously, the overall qualitative agreement is very good. At the resonant frequency f_{AFM} we observe an alternating pattern of the antisymmetric mode, whereas at the resonant frequency f_{FM} there are regular spots for the symmetric mode. It evidences clearly the difference between the AFM and FM orders of magnetic moments originated in the all-dielectric metasurface from the trapped mode splitting. We should note that the measured characteristic of the symmetric mode appears somewhat distorted. This is because at this resonant frequency the electromagnetic field is strongly confined inside the dielectric particles (which is specific for the trapped mode excitation). This brings some difficulties for the magnetic near-field probing.

V. STRONG POLARIZATION EFFECTS

It was previously discussed [41] that among all symmetries of the unit cells composed of four disks with eccentric through-hole, the metasurfaces whose unit cell corresponds to symmetries C_{4v} and C_4 are polarization insensitive. Moreover, among all these metasurfaces no polarization transformation was detected when considering unit cells with symmetries higher than C_1 . It is of interest to find out the polarization characteristics of the given metasurface whose unit cell belongs to the point group C_1 .

In Fig. 3(a) one can notice that the resonant curves of transmission and reflection spectra of diagonally polarized waves vary in the range from 0 to 1, since the material losses are excluded in this simulation. In the chosen frequency band the metasurface under study is almost transparent, whereas at the resonant frequencies f_{AFM} and f_{FM} it becomes reflective. In fact, both resonances acquire a sharp peak-and-trough (Fano) profile with variation between zero-transmission and zero-reflection which is typical for resonances originated from the trapped modes [27, 32].

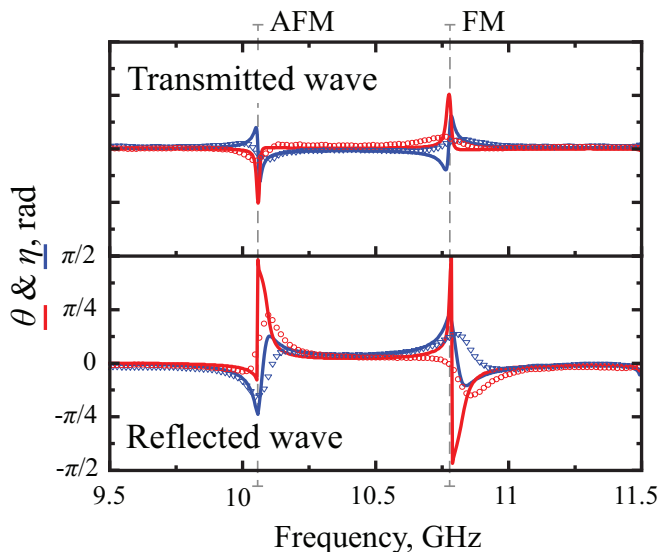


FIG. 5. Simulated (solid lines) and measured (scatters) polarization azimuth rotation angle θ and ellipticity angle η of the transmitted and reflected waves. In the simulation an ideal (lossless) metasurface is considered. All geometrical parameters of the metasurface are the same as in Fig. 1.

Contrariwise, the curves of transmission and reflection spectra of the horizontally and vertically polarized waves do not vary in the full range between 0 and 1, which may mean that the metasurface performs a polarization transformation. In order to reveal this feature, the cross-polarized components of the transmitted and reflected fields were additionally calculated. They appear to have nonzero values of the transmission and reflection at the corresponding resonant frequencies f_{AFM} and f_{FM} . With the co-polarized and cross-polarized components, the polarization state of both reflected and transmitted fields can be obtained using standard definitions [47]: $\tan 2\theta = U_2/U_1$ and $\sin 2\eta = U_3/U_0$, where θ is the polarization azimuthal angle and η is the ellipticity parameter. U_j ($j = 0, \dots, 3$) are the Stokes parameters calculated from the components of the electric field in the right-handed orthogonal frame. According to the definition of the Stokes parameters, we introduce the ellipticity η so that the field is linearly polarized when $\eta = 0$, and $\eta = -\pi/4$ for left-circular polarization and $+\pi/4$ for right-circular polarization. In cases with $0 < |\eta| < \pi/4$, the field is elliptically polarized. The frequency dependencies of both the polarization azimuth and ellipticity angle are summarized in Fig. 5.

Analyzing the properties of the transmitted and reflected fields, we note that generally the metasurface transforms a linearly polarized wave to an elliptically polarized wave in the narrow frequency band around the central resonant frequencies f_{AFM} and f_{FM} . There is a stronger polarization conversion in the reflected field where resonant values of the ellipticity angle reach $\pm\pi/4$ (so the reflected field becomes to be circularly polarized). The maximal azimuth rotation angle θ for the transmit-

ted field is $\pi/4$, whereas for the reflected field it is $\pi/2$. Thus, the metasurface can completely transform the reflected field into an orthogonally polarized wave with respect to the incident wave.

In order to verify this feature of the metasurface, a set of special measurements of polarization characteristics of the transmitted and reflected fields was conducted. For these experiments, the dielectric-lens antennas were rotated appropriately to measure the co-polarized and cross-polarized components of the transmitted and reflected spectra in the far field. The results on the polarization azimuth rotation angle and ellipticity angle are derived from the measured data and added in Fig. 5 as scatters. One can readily see reasonable agreement between simulations and measurements. Thus the experimental data support our theoretical finding concerning the effect of polarization transformation in the low-symmetry all-dielectric metasurface.

VI. CONCLUSIONS

Thus, by employing theoretical methods, numerical simulations, as well as far- and near-field microwave experimental studies, we have revealed and visualized experimentally novel physics of optically-induced magnetism in dielectric metasurfaces. More specifically, we have predicted the ordering of magnetic dipole moments with FM and AFM orders in low-symmetry all-dielectric metasurfaces and observed its experimental manifestation in strong polarization effects.

Our studies allow making the following conclusions: (i) both symmetric (FM) and antisymmetric (AFM) orders of optically-induced magnetic dipole moments can appear in low-symmetry all-dielectric metasurface composed of clusters of identical particles, and they do not require magnetic moments of different origin; (ii) both types of the magnetic orders originate from the splitting of the trapped mode whose excitation is supported by the asymmetric particles; (iii) horizontal and vertical linear polarizations acquire a substantial polarization rotation observed experimentally, where the metasurface can perform a complete polarization conversion of the reflected field into an orthogonally polarized wave.

In the proposed structures, we can gain an additional benefit associated with the excitation of the trapped mode. In particular, under the resonant conditions of the trapped-mode excitation, the electromagnetic field becomes strongly confined inside the structure, and this confinement depends on the degree of asymmetry of individual particles. Therefore, our metasurface can be employed as an efficient flat-optic platform for realizing enhanced light-matter interaction with metasurfaces.

ACKNOWLEDGMENTS

V.R.T. acknowledges a hospitality and financial support of the Jilin University; V.D. thanks the Brazilian Agency National Council of Technological and Scientific

Development (CNPq) for a financial support; Y.S.K. acknowledges a support from the Australian Research Council and useful discussions with Boris Luk'yanchuk.

-
- [1] L. D. Landau and E. M. Lifshitz, *Course of Theoretical Physics: Electrodynamics of Continuous Media*, 2nd ed., Vol. 8 (Butterworth-Heinemann, Oxford, 1984) Chap. 9.
 - [2] C. M. Soukoulis and M. Wegener, "Past achievements and future challenges in the development of three-dimensional photonic metamaterials," *Nat. Photonics* **5**, 523–530 (2011).
 - [3] F. Monticone and A. Alú, "The quest for optical magnetism: from split-ring resonators to plasmonic nanoparticles and nanoclusters," *J. Mater. Chem. C* **2**, 9059–9072 (2014).
 - [4] Y. Kivshar and A. P. Roberts, "Classical and exotic magnetism: Recent advances and perspectives," *Low Temp. Phys.* **43**, 895–900 (2017).
 - [5] J. B. Pendry, A. J. Holden, D. J. Robbins, and W. J. Stewart, "Magnetism from conductors and enhanced nonlinear phenomena," *IEEE Trans. Microwave Theory Techn.* **47**, 2075–2084 (1999).
 - [6] T. J. Yen, W. J. Padilla, N. Fang, D. C. Vier, D. R. Smith, J. B. Pendry, D. N. Basov, and X. Zhang, "Terahertz magnetic response from artificial materials," *Science* **303**, 1494–1496 (2004).
 - [7] S. Linden, C. Enkrich, M. Wegener, J. Zhou, Th. Koschny, and C. M. Soukoulis, "Magnetic response of metamaterials at 100 terahertz," *Science* **306**, 1351–1353 (2004).
 - [8] C. Enkrich, M. Wegener, S. Linden, S. Burger, L. Zschiedrich, F. Schmidt, J. F. Zhou, Th. Koschny, and C. M. Soukoulis, "Magnetic metamaterials at telecommunication and visible frequencies," *Phys. Rev. Lett.* **95**, 203901 (2005).
 - [9] B. Lahiri, S. G. McMeekin, A. Z. Khokhar, R. M. De La Rue, and N. P. Johnson, "Magnetic response of split ring resonators (SRRs) at visible frequencies," *Opt. Express* **18**, 3210–3218 (2010).
 - [10] V. M. Shalaev, W. Cai, U. K. Chettiar, H.-K. Yuan, A. K. Sarychev, V. P. Drachev, and A. V. Kildishev, "Negative index of refraction in optical metamaterials," *Opt. Lett.* **30**, 3356–3358 (2005).
 - [11] J. A. Fan, C. Wu, K. Bao, J. Bao, R. Bardhan, N. J. Halas, V. N. Manoharan, P. Nordlander, G. Shvets, and F. Capasso, "Self-assembled plasmonic nanoparticle clusters," *Science* **328**, 1135–1138 (2010).
 - [12] J. A. Fan, K. Bao, C. Wu, J. Bao, R. Bardhan, N. J. Halas, V. N. Manoharan, G. Shvets, P. Nordlander, and F. Capasso, "Fano-like interference in self-assembled plasmonic quadrumer clusters," *Nano Lett.* **10**, 4680–4685 (2010).
 - [13] L. Sun, T. Ma, S.-C. Yang, D.-K. Kim, G. Lee, J. Shi, I. Martinez, G.-R. Yi, G. Shvets, and X. Li, "Interplay between optical bianisotropy and magnetism in plasmonic metamolecules," *Nano Lett.* **16**, 4322–4328 (2016).
 - [14] W. Cai, U. K. Chettiar, H.-K. Yuan, V. C. de Silva, A. V. Kildishev, V. P. Drachev, and V. M. Shalaev, "Metamagnetics with rainbow colors," *Opt. Express* **15**, 3333–3341 (2007).
 - [15] H.-K. Yuan, U. K. Chettiar, W. Cai, A. V. Kildishev, A. Boltasseva, V. P. Drachev, and V. M. Shalaev, "A negative permeability material at red light," *Opt. Express* **15**, 1076–1083 (2007).
 - [16] T. Pakizeh, A. Dmitriev, M. S. Abrishamian, N. Granpayeh, and M. Käll, "Structural asymmetry and induced optical magnetism in plasmonic nanosandwiches," *J. Opt. Soc. Am. B* **25**, 659–667 (2008).
 - [17] M. W. Klein, C. Enkrich, M. Wegener, C. M. Soukoulis, and S. Linden, "Single-slit split-ring resonators at optical frequencies: limits of size scaling," *Opt. Lett.* **31**, 1259–1261 (2006).
 - [18] A. I. Kuznetsov, A. E. Miroshnichenko, M. L. Brongersma, Y. S. Kivshar, and B. Luk'yanchuk, "Optically resonant dielectric nanostructures," *Science* **354**, aag2472 (2016).
 - [19] S. Kruk and Y. Kivshar, "Functional meta-optics and nanophotonics governed by Mie resonances," *ACS Photonics* **4**, 2638–2649 (2017).
 - [20] Y. Kivshar, "All-dielectric meta-optics and non-linear nanophotonics," *Natl Sci. Rev.* **5**, 144–158 (2018).
 - [21] Q. Zhao, J. Zhou, F. Zhang, and D. Lippens, "Mie resonance-based dielectric metamaterials," *Mater. Today* **12**, 60–69 (2009).
 - [22] A. E. Miroshnichenko, B. Luk'yanchuk, S. A. Maier, and Y. S. Kivshar, "Optically induced interaction of magnetic moments in hybrid metamaterials," *ACS Nano* **6**, 837–842 (2012).
 - [23] A. E. Miroshnichenko, D. Filonov, D. Lukyanchuk, and Y. Kivshar, "Antiferromagnetic order in hybrid electromagnetic metamaterials," *New J. Phys.* **19**, 083013 (2017).
 - [24] S. Lepeshov and Y. Kivshar, "Near-field coupling effects in Mie-resonant photonic structures and all-dielectric metasurfaces," *ACS Photonics* **5**, 2888–2894 (2018).
 - [25] K. Koshelev, S. Lepeshov, M. Liu, A. Bogdanov, and Y. Kivshar, "Asymmetric metasurfaces with high-*Q* resonances governed by bound states in the continuum," *Phys. Rev. Lett.* **121**, 193903 (2018).
 - [26] K. Koshelev, A. Bogdanov, and Y. Kivshar, "Meta-optics and bound states in the continuum," *Sci. Bull.* **64**, 836–842 (2019).
 - [27] V. A. Fedotov, M. Rose, S. L. Prosvirnin, N. Papasimakis, and N. I. Zheludev, "Sharp trapped-mode resonances in planar metamaterials with a broken structural symmetry," *Phys. Rev. Lett.* **99**, 147401 (2007).
 - [28] E. Plum, V. A. Fedotov, P. Kuo, D. P. Tsai, and N. I. Zheludev, "Towards the lasing spaser: controlling metamaterial optical response with semiconductor quantum dots," *Opt. Express* **17**, 8548–8551 (2009).
 - [29] V. V. Khardikov, E. O. Iarkov, and S. L. Prosvirnin, "Trapping of light by metal arrays," *J. Opt.* **12**, 045102 (2010).

- (2010).
- [30] V. V. Khardikov, E. O. Iarko, and S. L. Prosvirnin, “A giant red shift and enhancement of the light confinement in a planar array of dielectric bars,” *J. Opt.* **14**, 035103 (2012).
 - [31] A. Jain, P. Moitra, T. Koschny, J. Valentine, and C. M. Soukoulis, “Electric and magnetic response in dielectric dark states for low loss subwavelength optical meta atoms,” *Adv. Opt. Mater.* **3**, 1431–1438 (2015).
 - [32] V. R. Tuz, V. V. Khardikov, A. S. Kupriianov, K. L. Domina, S. Xu, H. Wang, and H.-B. Sun, “High-quality trapped modes in all-dielectric metamaterials,” *Opt. Express* **26**, 2905–2916 (2018).
 - [33] C. Cui, C. Zhou, S. Yuan, X. Qiu, L. Zhu, Y. Wang, Y. Li, J. Song, Q. Huang, Y. Wang, C. Zeng, and J. Xia, “Multiple Fano resonances in symmetry-breaking silicon metasurface for manipulating light emission,” *ACS Photonics* **5**, 4074–4080 (2018).
 - [34] A. Sayanskiy, A. S. Kupriianov, S. Xu, P. Kapitanova, V. Dmitriev, V. V. Khardikov, and V. R. Tuz, “Controlling high- Q trapped modes in polarization-insensitive all-dielectric metasurfaces,” *Phys. Rev. B* **99**, 085306 (2019).
 - [35] M. Decker, S. Burger, S. Linden, and M. Wegener, “Magnetization waves in split-ring-resonator arrays: Evidence for retardation effects,” *Phys. Rev. B* **80**, 193102 (2009).
 - [36] M. Decker, S. Linden, and M. Wegener, “Coupling effects in low-symmetry planar split-ring resonator arrays,” *Opt. Lett.* **34**, 1579–1581 (2009).
 - [37] N. Born, I. Al-Naib, C. Jansen, T. Ozaki, R. Morandotti, and M. Koch, “Excitation of multiple trapped eigenmodes in terahertz metamolecule lattices,” *Appl. Phys. Lett.* **104**, 101107 (2014).
 - [38] L. Cong, V. Savinov, Y. K. Srivastava, S. Han, and R. Singh, “A metamaterial analog of the Ising model,” *Adv. Mater.* **30**, 1804210 (2018).
 - [39] A. A. Barybin and V. A. Dmitriev, *Modern Electrodynamics and Coupled-Mode Theory: Application to Guided-Wave Optics* (Rinton Press Princeton, New Jersey, 2002).
 - [40] R. K. Mongia and P. Bhartia, “Dielectric resonator antennas - A review and general design relations for resonant frequency and bandwidth,” *Int. J. RF Microw. Comput. Aided Eng.* **4**, 230–247 (1994).
 - [41] P. Yu, A. Kupriianov, V. Dmitriev, and V. Tuz, “All-dielectric metasurfaces with trapped modes: Group-theoretical description,” *J. Appl. Phys.* **125**, 143101 (2019).
 - [42] V. Dmitriev, “Symmetry properties of electromagnetic planar arrays: Long-wave approximation and normal incidence,” *Metamaterials* **5**, 14–148 (2011).
 - [43] “Frequency selective surface, periodic complementary split ring resonator,” *Comsol Application Gallery* ID: 15711.
 - [44] X. Liu, K. Fan, I. V. Shadrivov, and W. J. Padilla, “Experimental realization of a terahertz all-dielectric metasurface absorber,” *Opt. Express* **25**, 191–201 (2017).
 - [45] D. Diessel, M. Decker, S. Linden, and M. Wegener, “Near-field optical experiments on low-symmetry split-ring-resonator arrays,” *Opt. Lett.* **35**, 3661–3663 (2010).
 - [46] S. Xu, A. Sayanskiy, A. S. Kupriianov, V. R. Tuz, P. Kapitanova, H.-B. Sun, W. Han, and Y. S. Kivshar, “Experimental observation of toroidal dipole modes in all-dielectric metasurfaces,” *Adv. Opt. Mater.* **7**, 1801166 (2019).
 - [47] E. Collett, *Polarized Light: Fundamentals and Applications* (Dekker, New York, 1993).